International Journal of Engineering and Applied Sciences (IJEAS)
Vol.2, Issue 1(2010)16-26

NUMERICAL COMPUTATION OF FLUID FLOW AND AEROSOL TRANSPORT IN A LONG ELECTRICAL MOBILITY SPECTROMETER

P. Intra[1]*, L.P. Purba[2], N. Tippayawong[3]
[1] College of Integrated Science and Technology, Rajamangala University of Technology Lanna, Chiang Mai, Thailand 50300
[2] Department of Mechanical Engineering, Prince of Songkla University, Hat Yai, Thailand 90110
[3] Department of Mechanical Engineering, Chiang Mai University, Chiang Mai, Thailand 50200
*Corresponding Author: E-mail: panich_intra@yahoo.com

Accepted Date: 12 July 2009

Abstract

Size distribution of submicron airborne particles can be effectively determined using electrical mobility technique. In this study, a numerical computation model for prediction of fluid flow and aerosol transport in a long column, electrical mobility spectrometer (EMS) has been developed. The internal 3D structure of an EMS [Intra and Tippayawong (2009), Korean J. Chem. Eng., 26(1), 269] was employed to simulate the complex flow patterns and aerosol particle trajectories in the EMS, including the swirling flow developed near the sheath air inlet slit. The incompressible Navier-Stokes equations were numerically calculated for the gas flow and particle trajectories, with a commercial computational fluid dynamics software package, FLUENT 6.3. The calculated results were found to agree well with previously published results in the literature. Prediction of fluid flow and aerosol transport was particularly useful in the EMS design and development.

Keywords: Aerosol, Particle, Numerical Simulation, Electrical Mobility, Spectrometer

1. Introduction

A long column, electrical mobility spectrometer (EMS) or a multi-channel differential mobility analyzer (DMA) is increasingly becoming one of the most commonly used instruments for the classification and measurement of aerosol particle size distribution in the nanometer-sized range because of its better time response than a typical DMA. The most widely used EMS is based on the design developed by Mirme [1]. Intra and Tippayawong [2] offers a review of the recent development of this technique.

A typical EMS consists of two concentric electrodes between which a potential is applied. There are two streams; polydisperse aerosol and sheath air flows. The inner electrode of the spectrometer is maintained at a DC high voltage while the outer chassis of the spectrometer is grounded. The charged particles enter the spectrometer column close to the inner electrode by a continuous flow of air, and surrounded by a sheath air flow. Since the inner electrode is kept at a high voltage, the charged particles are deflected outward in a radial direction. They are collected on a series of electrically isolated electrometer rings positioned at the inner surface of the outer chassis of the spectrometer column. Virtual ground potential input of highly sensitive electrometers are connected to these electrometer rings to measure currents corresponding to the number concentration of particles in a given mobility which is in turn related to the particle size distribution. Resolution of the instrument is determined mainly by the number and width of the electrometer rings. The size range of particle collected

on the electrometer rings can be varied by adjusting the aerosol and sheath air flow rates, the voltage applied to the inner electrode, and the operating pressure.
It is well known that fluid flow and particle transport inside the EMS are important factors influencing accurate particle size distribution measurements. Fluid flow condition in the EMS is designed to be in the laminar regime. Turbulent mixing which can deteriorate the EMS performance should be avoided. However, depending on the flow conditions of sheath air and aerosol inlet, the flow may become turbulent. With regards to sizing ultrafine aerosol particles of diameter smaller than a few tens of nm, Brownian diffusion motion becomes important [3, 4]. Fluid flow and particle transport inside a DMA has been studied by many people [5 – 9]. Very few studies have been done on the EMS [10]. To our knowledge, investigation of a 3D simulation of fluid flow and particle transport in the long column EMS is even less. In this paper, a 3D computational model for prediction of fluid flow and aerosol particle transport inside a long EMS was developed and studied. A detailed description of the operating principle of the EMS was also presented.

2. Description of a Long EMS

The EMS has one long column, consisting of coaxially cylindrical electrodes. Fig. 1 shows a schematic diagram of the long EMS used in this study [4]. Outer chassis was made of a 481 mm long aluminum tube with an internal diameter of 55 mm. Inner electrode was made of a 25 mm in diameter stainless steel rod. Width of the aerosol inlet channel was 2 mm. It is important to ensure that flow is laminar inside the EMS column. The sheath-air flow entered with a swirl component and then flowed through a 0.1 mm thick Teflon mesh to ensure the flow was laminar. The 22 electrometer rings used resulted in the classification of every measured aerosols into 22 mobility ranges. The electrometer rings have a width of 19 mm. The first electrometer ring was located 20 mm downstream the aerosol inlet, while a 1 mm gap was allowed between the electrometer rings for electrical isolation.

3. Physical Modeling

Gas flow and particle motion were numerically modeled and solved to estimate the particle transport in the long EMS.

3.1 Gas continuity

The gas flow was considered as the main phase and its motion was described by the continuity and momentum equations, known as the Navier-Stokes equations;

$$\frac{\partial}{\partial x_k}(r u_k) = 0 \tag{1}$$

$$\frac{\partial}{\partial x_k}\left(r u_i u_k - (m + m_t)\frac{\partial u_k}{\partial x_k} \right) = -\frac{\partial p}{\partial x_i} + f_{D_i} \tag{2}$$

where r is the gas density, and u_k is the gas velocity component in the x_k direction, m is the gas molecular dynamic viscosity, f_{D_i} is the aerodynamic drag force, and p is the gas pressure.

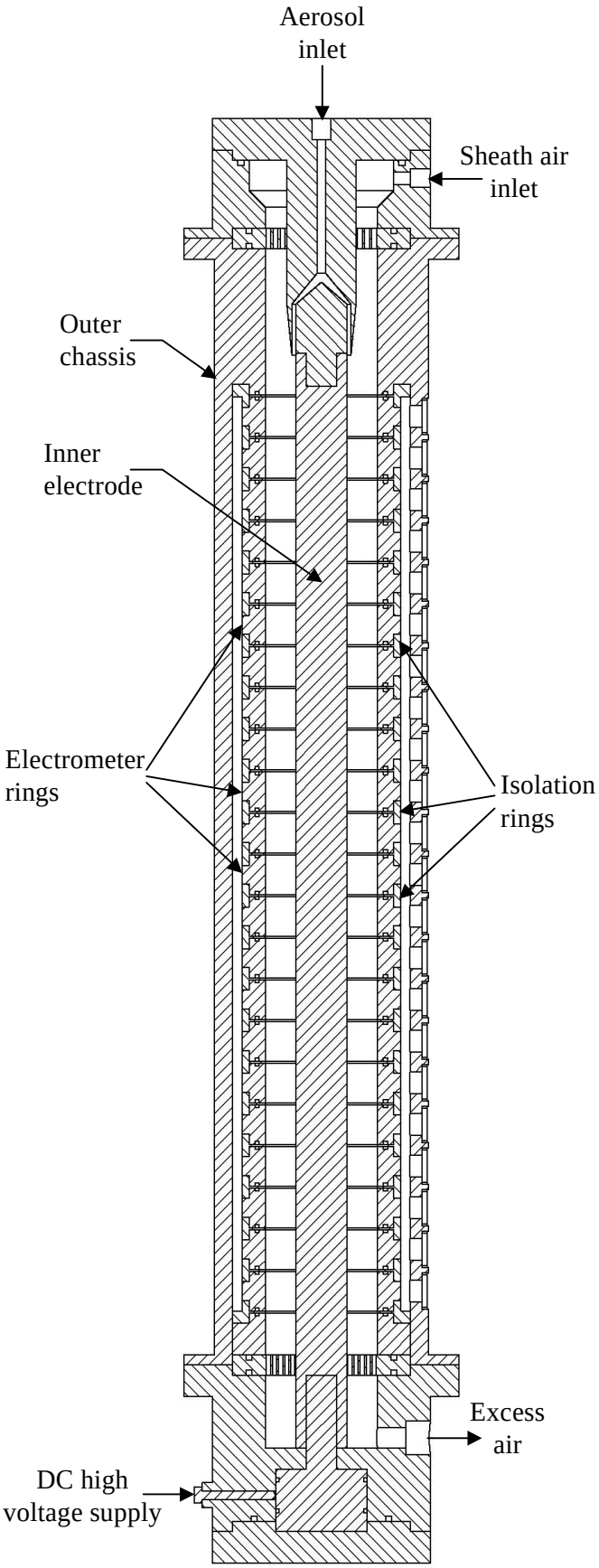

Fig. 1. Schematic diagram of the long EMS [1]

3.2 Particle motion

Aerosol particles were decelerated by aerodynamic drag. Collision and coagulation between particles were neglected. The equation of the particle motion was expressed as:

$$\frac{\mathrm{d}x_i}{\mathrm{d}t} = v_i \tag{3}$$

$$m_p \frac{dv_i}{dt} = \frac{1}{C_c} 3pmd_p(u_i - v_i) \tag{4}$$

where m_p is the particle mass, v_i is the particle velocity, C_c is the Cunningham correction factor, and d_p is the particle diameter.

4. Numerical Computation

4.1. Calculation procedure

Fluid flow and particle trajectories in an internal 3D structure of the EMS were calculated with the commercial CFD package, FLUENT 6.3, using a finite volume method for solving the incompressible Navier-Stokes equations in cylindrical coordinates. The solution domain was divided into a number of cells. In the finite volume approach of FLUENT 6.3, the governing equations for the gas flow and the particles motion were numerically integrated over each of these computational cells.

4.2. Boundary conditions

The computational domain of the EMS is shown in Fig. 2. The modeled EMS consisted of the aerosol and sheath air inlets, and outlet boundaries. No slip boundary was applied to all the solid walls included in the computation domain, and fixed velocity boundary conditions were applied to the aerosol and sheath air flow inlets. The velocities at each inlet were calculated from the flow rates through these slits. Uniform velocity profile was assumed at the sheath and aerosol inlets across the cross section of the inlet tubes. Boundary conditions used in this calculation are summarized in Table 1.

4.3. Computational mesh

Fig. 3 shows a computational mesh used for the fluid flow and particle transport simulations. The grid generation program, GAMBIT, was used to construct the grid system of this model. Finer grids were used in the region close to the aerosol entrance and where the velocity gradient was expected to be large. An unstructured mesh was used. A total of about 869,401 meshes were distributed in the computational domain of internal flows in the EMS.

5. Results and Discussion

The operating gas was ambient air (density is 1.225 kg/m^3 and viscosity is 1.7894×10^{-5} kg/m/s), while particle diameter was between 10 – 1000 nm. Fig. 4 shows CFD results of the fluid velocity distribution in the EMS. High towards low intensity regions were indicated by red, yellow, green to blue, respectively.

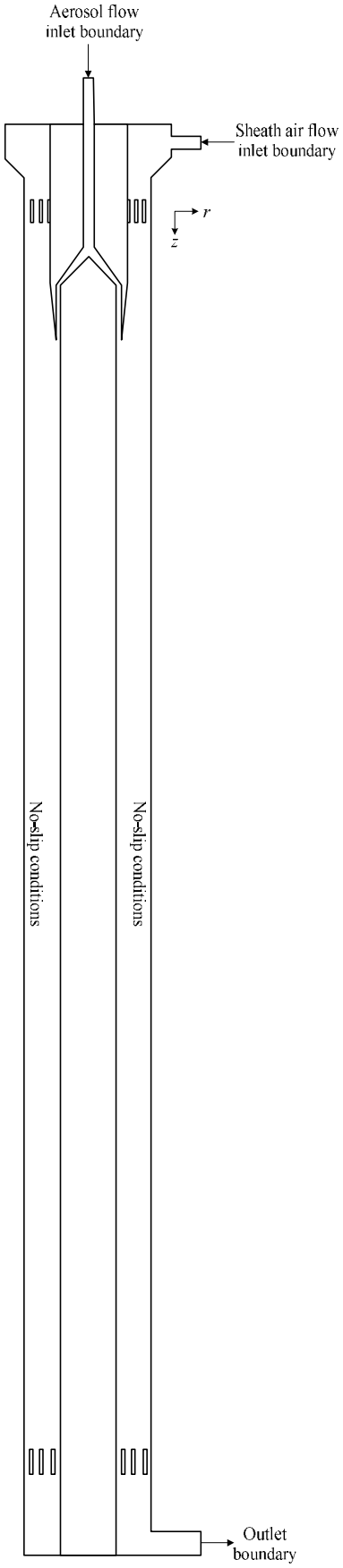

Fig. 2. Computational domain of the EMS

Table 1. Boundary conditions for CFD calculation

Air velocity at aerosol inlet	u_r = 0.0 m/s
	u_x = 0.0 m/s
	u_z = 0.106 m/s
Air velocity at sheath air inlet	u_r = 7.43 m/s
	u_x = 0.0 m/s
Air velocity at outlet	u_z = 0.0 m/s
Inner electrode	mass conservation
Electrometer rings	no slip
Insulator rings	no slip
	no slip

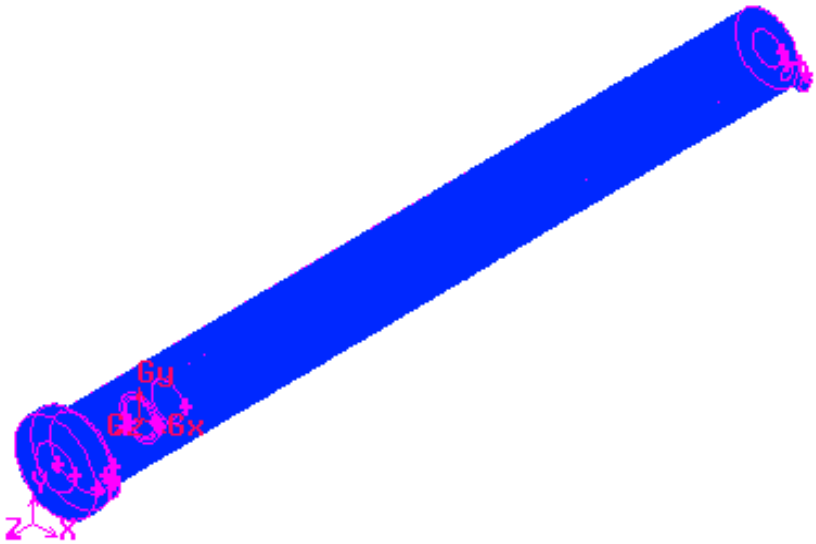

(a) Total view

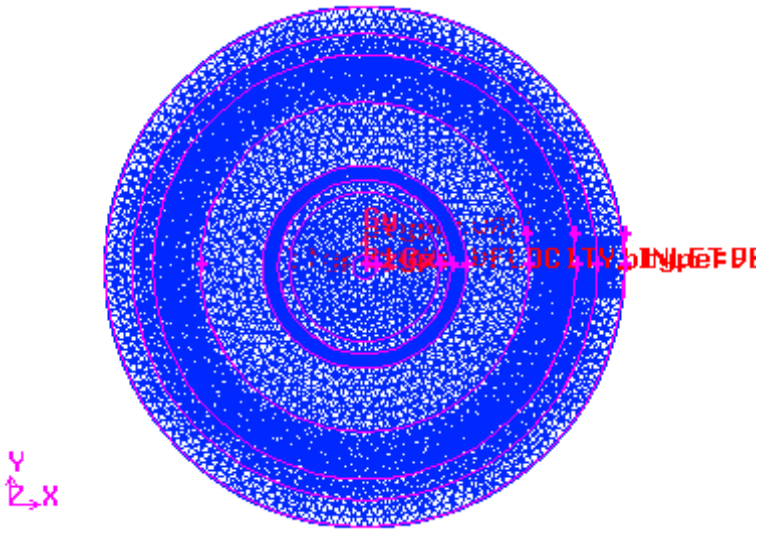

(b) Cross section view

Fig. 3. Computational mesh of the EMS

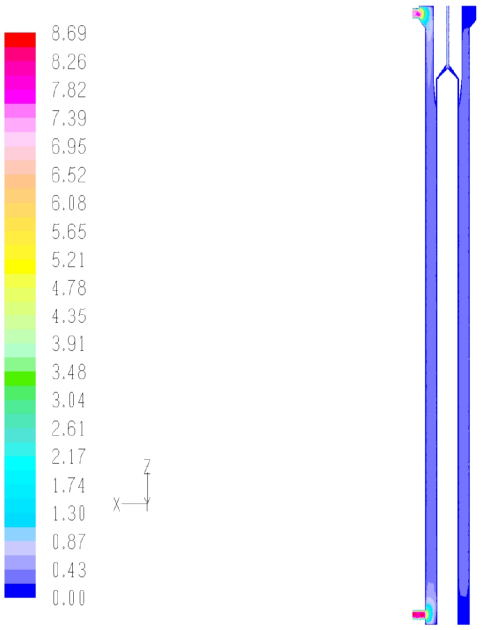

(a) Total view

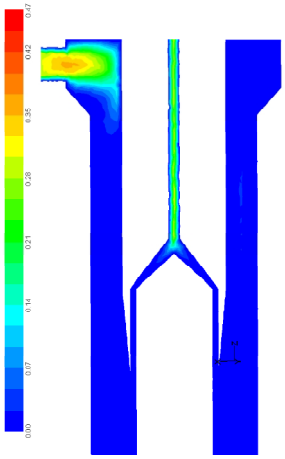

(b) The regions close to aerosol and sheath air inlets

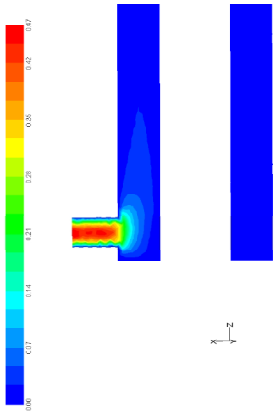

(c) The regions close to excess air outlet

Fig. 4. CFD calculations of the fluid flow velocity inside the EMS

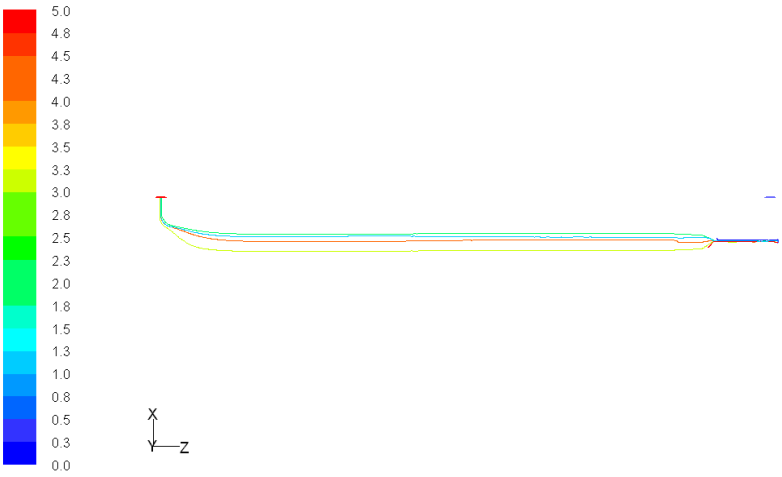

(a) Aerosol inlet

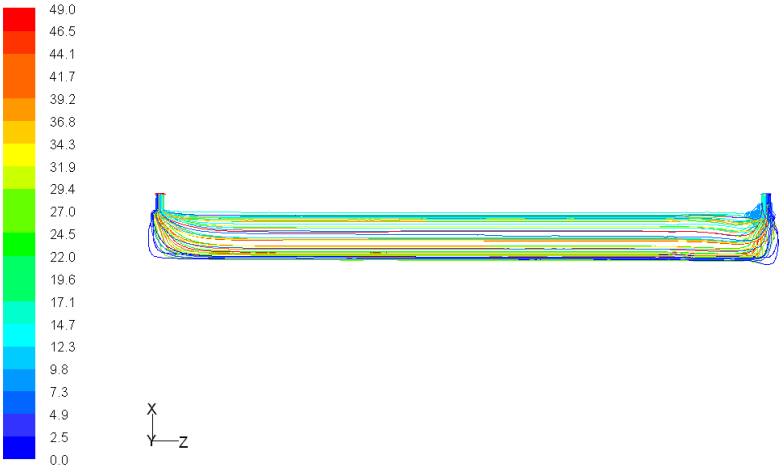

(b) Sheath air inlet

Fig. 5. CFD calculations of the mass less particle trajectories from (a) aerosol inlet and (b) sheath air inlet

Fig. 4(b) shows the detailed flow matching condition around the aerosol and sheath air inlets. Non-uniform flow velocity distribution was found near the aerosol and sheath air inlet boundaries. In general, the flow profile became fully developed at a few hydraulic diameters downstream from the aerosol inlet, while negligible disturbances occurred at the point where the two flows (aerosol and sheath air) merged. Fig. 4(c) shows the detailed flow velocity around the excess air outlet. It can be seen that the highest flow velocity was found in the excess air outlet, located in the bottom left corner side of the model. Flow simulation results showed qualitatively similar trend to those by the previous published results in the literature [5, 10]. Fig. 5 shows CFD calculation results of massless particle trajectories inside the EMS. The massless particles entered from aerosol and sheath air inlets to excess air outlet. Figs. 6(b) and 6(c) shows trajectories of massless particles around the aerosol and sheath air inlets, and excess air outlet. Uniform distribution of particles was observed downstream from the aerosol and sheath air inlets. It was also shown that the non-uniformity of particle circumferential distribution that existed near the aerosol and sheath air inlets and excess air outlet was caused by a non-uniform gas velocity distribution in the vicinity of the aerosol and sheath air inlets. Since the aerosol entered into the EMS column through a narrow annular slit, the EMS transmission efficiency dropped significantly for particles below 10 nm due to diffusion losses in the annulus and other flow passages. Furthermore, long residence time in the EMS

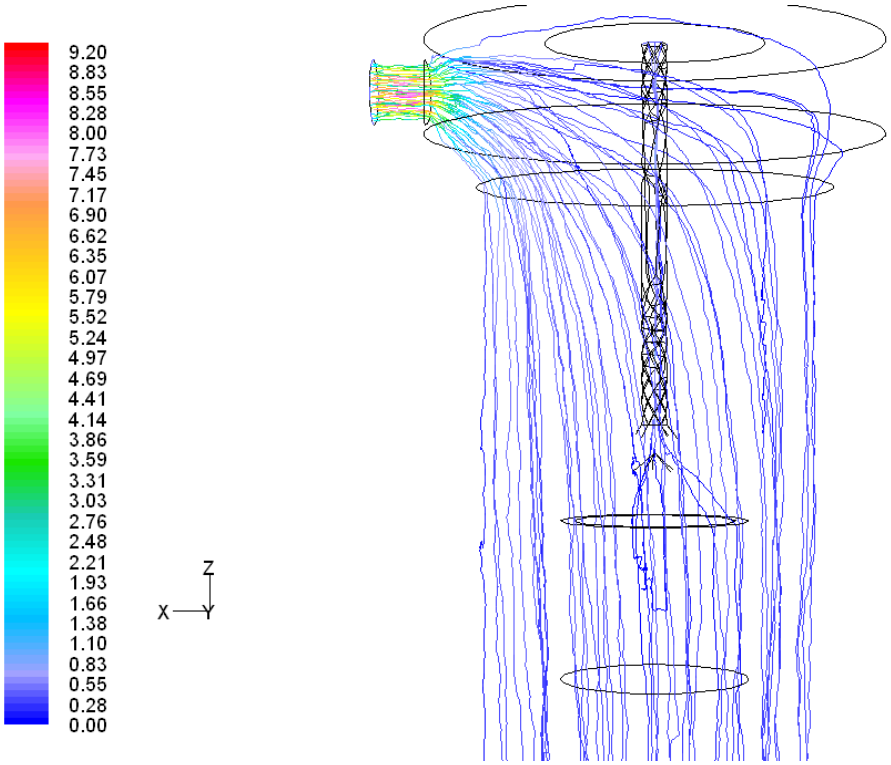

(a) The regions close to aerosol and sheath air inlets

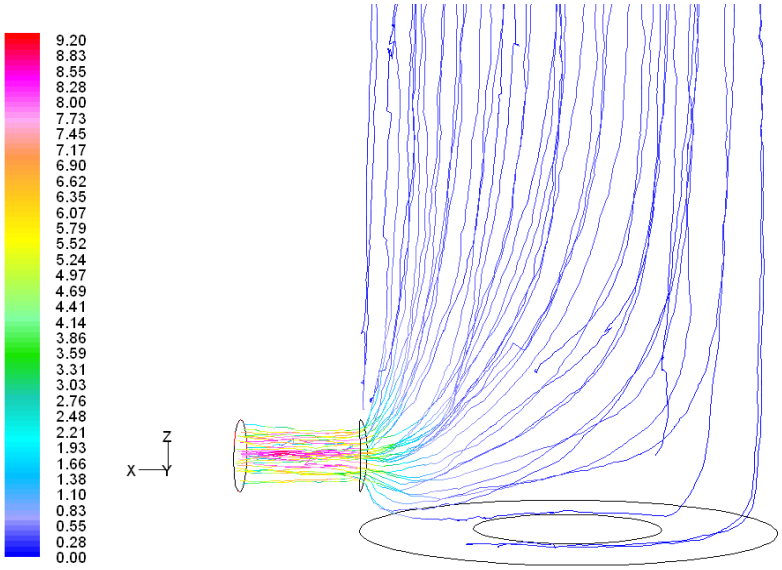

(b) The regions close to excess air outlet

Fig. 6. CFD calculations of the massless particle trajectories inside the EMS

column region resulted in substantial Brownian diffusion broadening of the transfer function for nanometer-sized particles. Fig. 7 shows particle trajectories in the EMS, taking into account the Brownian diffusion effect for particle diameters of 10, 100, and 1000 nm. It was shown that particles larger than 10 nm were found to exhibit lower Brownian diffusive motion than 10 nm particle. It was apparent that Brownian diffusion influenced particle trajectories significantly when the particle diameter was smaller than 10 nm [3, 4]. CFD results confirmed similarity with the previous work [4].

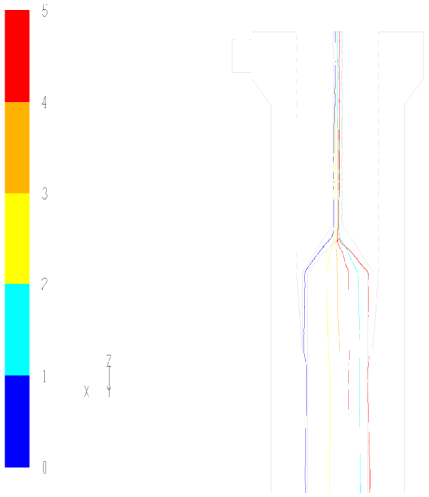

(a) 10 nm

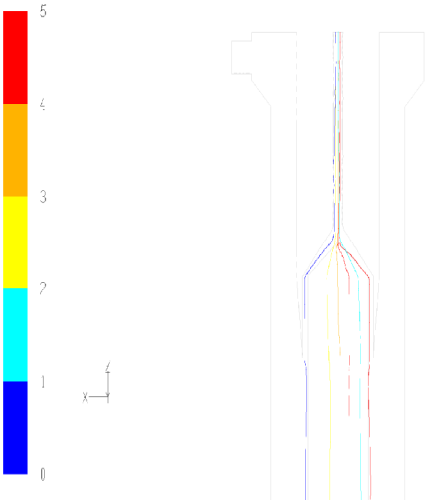

(b) 100 nm

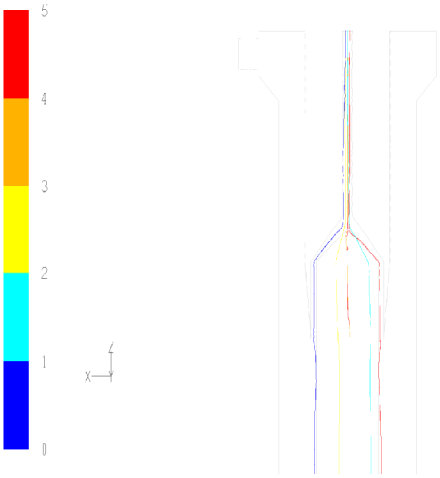

(c) 1000 nm

Fig. 7. CFD calculations of the particle trajectories inside the EMS

6. Conclusions

A 3D numerical model was developed for the description of fluid flow and aerosol particle transport inside the long EMS. The model was developed with the commercial CFD package, FLUENT 6.3. The model was extensively applied to 3D geometry provided with detailed gas flow field, and particle trajectories. It was shown that the numerical simulation results exhibited a qualitatively well-agreed trend with the published results in the literature. It has been demonstrated here that a numerical model can be used to predict flow field and particle transport, hence, assist in designing an EMS for nanometer-sized aerosol particle measurement. For future study, an experimental validation was also planned.

Acknowledgement

The authors wish to express their gratitude to the National Electronic and Computer Technology Center, Thailand for their support (contract no. NT-B-22-SS-11-50-18).

References

[1] Mirme, A., Electric Aerosol Spectrometry, Ph.D. Thesis, University of Tartuensis, Tartu, Estonia, 1994.

[2] Intra, P. and Tippayawong, N., An overview of differential mobility analyzers for size classification of nanometer-sized aerosol particles, *Songklanakarin J. Sci. Technol.*, 30, 243-256, 2008.

[3] Kousaka, Y., Okuyama, K., Adachi, M. and Mimura, T., Effect of Brownian diffusion on electrical classification of ultrafine aerosol particles in differential mobility analyzer, *J. Chem. Eng. Japan.*, 19, 401-407, 1986.

[4] Intra, P. and Tippayawong, N., Analysis of Brownian diffusion effect on nanometer aerosol classification in electrical mobility spectrometer, *Korean J. Chem. Eng.*, 26, 269-276, 2009.

[5] Chen, D. R. and Pui, D.Y.H., Numerical modeling of the performance of differential mobility analyzer for nanometer aerosol measurements, *J. Aerosol Sci.*, 28, 985-1004, 1997.

[6] Otani, Y., Emi, H., Cho, S. and Okuyama, K., Technique for aerosol flow check in differential mobility analyzer and its influence on classification performance, *J. Chem. Eng. Japan.*, 30, 1065-1069, 1997.

[7] Chen, D. R., Pui, D.Y.H., Hummes, D., Fissan, H., Quant, F. R. and Sem, G. J., Design and evaluation of a nanometer aerosol differential mobility analyzer (nano-DMA), *J. Aerosol Sci.*, 29, 497-509, 1998.

[8] Chen, D. R., Pui, D.Y.H., Mulholland, G. W. and Fernandez, M., Design and testing of an aerosol/sheath inlet for high resolution measurements with a DMA, *J. Aerosol Sci.*, 30, 983-999, 1999.

[9] Asai, T., Shimada, M., Okuyama, K., Kim, T. and Komatsubara, M., Numerical simulation on the effect of internal geometry and operating conditions on particle concentration distribution within a differential mobility analyzer, *J. Aerosol Res.*, 12, 145-153, 1999.

[10] Intra, P. and Tippayawong, N., Numerical simulation of flow and electric fields in an electrical mobility spectrometer, *International Symposium on Nanotechnology in Environmental Protection and Pollution*, Bangkok, Thailand, 2005.